Preparation and dielectric spectroscopy characterization of lyotropic liquid crystal materials

A Thesis Submitted in partial fulfillment

Of

The requirement for the award of the degree

Of

MASTER OF TECHNOLOGY (M. Tech)

In

Materials & Metallurgical Engineering
By

Ihab fathi Ayoob
Roll No. 601002006

SCHOOL OF PHYSICS & MATERIAL SCIENCE
THAPAR UNIVERSITY
PATIALA -147004, INDIA

2012

Dedicated
To
My Parents

THAPAR UNIVERSITY

PATIALA (PUNJAB)-147004 INDIA
June 2012

CERTIFICATE

This is to certify that the thesis entitled **"Preparation and dielectric spectroscopy characterization of lyotropic liquid crystal materials"** which is being submitted by **Ihab Fathi Ayoob** in Partial fulfillment of the requirements for the award of the degree of ***Master of Technology (M.Tech.) in Materials & Metallurgical Engineering*** of Thapar University, Patiala (India), is a record of the study conducted by him under my supervision and guidance and that no part of this thesis has been submitted for the award of any other degree.

(Dr. K.K. Raina)

Distinguish Professor and Deputy Director
Thapar University
Patiala, Punjab (147004)

Date:
Place: Patiala

COUNTERSIGNED

(Dr. Kulvir Singh)

(Associate Professor and Head)
School of Physics & Material Sciences
Thapar University, Patiala

(

Dean, Academic Affairs
Thapar University, Patiala

ACKNOWLEDGEMENTS

I am extremely thankful to **Dr. K.K. Raina** *Distinguish Professor and Deputy Director Thapar University, (Patiala), my guide for giving me a chance to work in his supervision and without whose help and constant guidance this thesis would have not taken shape. I shall always treasure his affectionate guidance, wholehearted co-operation and constructive suggestions during the present study.*

I am grateful to **Dr. Kulvir Singh**, *Associate Professor and Head, School of Physics and Materials Science for his encouragement and execution of report work.*

I would also like to thank **Dr. O.P. Pandey,** *Sr. Professor, School of Physics and Materials Science for his constant guidance and encouragement.*

It gives me immense pleasure to express my special thanks to **Dr. Puneet Sharma**, *Assistant Professor who always took keen interest in guiding me during my work.*

I wish my sincere thanks to **Dr. Bhupendrakumar Chudasama**, *Assistant Professor who always took keen interest in guiding me during my work.*

It was a pleasure to be in a very nice group at MRL (Material Research Laboratory).I would like to thank all the members of the group for a pleasant working atmosphere and especially **Mr. Ravi K. Shukla, Mr. Rishi, Ms.Gurpreet K. Bhullar and Ms. Ramneek Kaur** *Ph.D students who's helping me in this report and also in practical work.*

I owe my sincere thanks to all the staff members of School of Physics and Materials Science for their support and encouragement who never turned me down whenever I approached for any help.

I also wanted to thank my family who inspired, encouraged and fully supported me in every trial that came my way. Also, I thank them for giving us not just financial, but moral and spiritual support.

Ihab Fathi Ayoob
Roll No. 601002006

Contents

List of symbols and abbreviation

LLC	**Lyotropic liquid crystal**
H_1	**Direct hexagonal phase**
H_2	**Inverted hexagonal phase**
Lα	**Lamellar neat phase**
Pβ'	**Lamellar ripple phase**
I_1	**Direct micelles**
I_2	**Reversed micelles**
CMC	**Critical micellar concentration**
CTAB	**Cetyltrimethylammonium bromide**
SDS	**Sodium dodecylsulfate**
DSC	**Differential Scanning Calorimetry**
ITO	**Indium tin oxide**
RCL	**Inductance Capacitance Resistance**
ε'	**Dielectric permittivity**
ε"	**Loss**
ε*	**complex dielectric permittivity**

List of Figures

List of Tables

Abstract

Five samples of lyotropic liquid crystals of SDS/CTAB/water have been prepared, in different concentration. These samples were characterized by thermal polarizing microscopy for morphological, thermo-optical studies. The dielectric spectroscopy measurements were carried out in a wide frequency range 50Hz to 1 MHz by RCL meter. Sample show higher dielectric permittivity in the lower frequency. Large dispersion in permittivity has been observed in these systems at the expense of temperature variation in the frequency dependent studies, which may be associated with the change in the optimal area and ordering of the micelles. The temperature dependent dielectric studies reflect the decrease in the permittivity with the increment in the temperature however fluctuation near 60^0C owes to the phase transition. The ternary systems exhibit thermal hysteresis attributed to the unpacking of LLC structures to the micellar phase. These systems of materials are expected to find wide range of applications including their use in electrolytic capacitors and energy storage devices.

CHAPTER 1

Introduction and Review of literature

Liquid crystals are intermediate states of matter, between an isotropic liquid and a solid crystalline. This leads to the concept of ordering in soft materials. These molecule, display orientantional order and even positional order along some specific directions. These materials flow like an isotropic fluid and have characteristic optical properties of solid crystals [1]. The liquid crystallinity or mesomorphic behavior was first observed by Reinitzer (1888) and Lehmann (1889) [2].

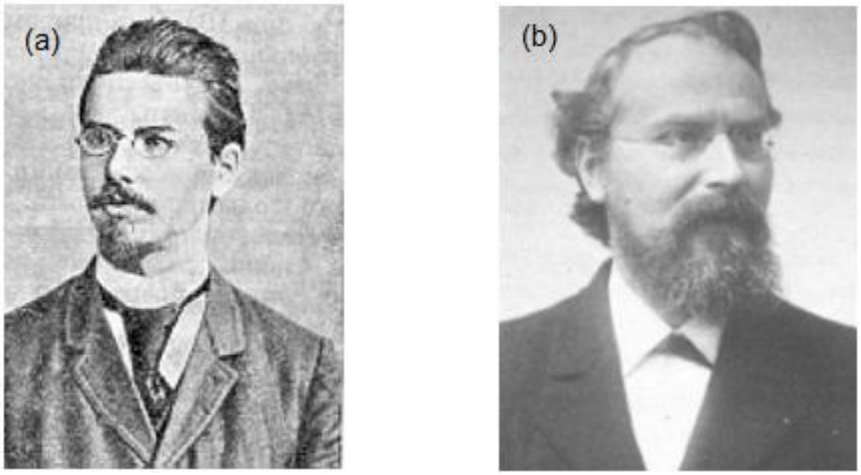

Figure 1.1: discover of liquid crystal (a) Fredrich Reinitzer (1857-1927) and (b) Otto Lehmann (1855-1922).

1.1 Liquid crystals classification

Liquid crystals are classified as Thermotropics and lyotropics, depending on the physico-chemical parameters responsible for the phase transitions [1].

1.1.1 Thermotropic liquid crystal

In these systems of organic molecules, phase transitions depend on temperature and pressure. Pronounced shape anisotropy (in other words, the anisometry) is the main feature of the molecules which give rise to a thermotropic mesophase. Rods, discs, and banana-shaped are examples of molecular geometries associated with thermotropic liquid crystals. Some thermotropic liquid crystal molecules show orientation order only like a nematic phase whereas others may show both position and orientation order like smectic A and smectic C. Besides pure substances, mixtures of these molecules can also exhibit thermotropic mesomorphic properties. Thermotropics are widely used in displays for low power consumption and in many sensor devices [1, 3-4].

1.1.2 Lyotropic liquid crystals

Lyotropic liquid crystals, shortly called lyotropics or lyomesophases, are mixtures of amphiphilic molecules and solvents at given temperature and relative concentrations. The mesomorphic properties change with temperature, pressure and the relative concentrations of the different components of the mixture. An important feature of lyotropics is it's self-assembly in different structures of amphiphilic molecules in solvent, which are the basic units of these mesophases [1]. Lyotropic liquid crystals are formed on the dissolution of most surfactants in a solvent (usually water). Surfactants are amphiphilic materials whose constituent molecules are formed from a hydrophilic polar

head group and a hydrophobic tail chain (often hydrocarbon) [5]. The concepts hydrophobic (hates water) and hydrophilic (loves water) refer to the affinity of a particular molecule with respect to the water molecules [1]. There exists several different types of lyotropic liquid crystal structures which possess a different arrangement of molecules within the solvent matrix. The concentration of the solute material in the solvent determines the kinds of lyotropic liquid crystal phase are exhibits. However, at a given concentration, it is also possible to observe transitions between lyotropic mesophases by changing the temperature [5]. And accordingly we can classify the amphiphilic molecules into:

- Anionic surfactants
- Cationic Surfactants
- Non-ionic Surfactants
- Zwitterionic Surfactants

1.2 Structure of lyotropic liquid crystals :

Water is present in almost all of lyotropic mixtures. The behavior of a molecule of a given substance with respect to the water molecules plays a crucial role in the formation of a lyomesophases. Amphiphilic compounds are highly polar in nature. Their liquid crystalline behavior can be characterized by a segregation of the polar and the non polar parts of the molecules. There are well known lamellar, hexagonal and cubic phases reported in the literature. The first two have a single symmetry axis, while the symmetry of the cubic phases is obvious from the nomenclature. These exist several different types of lyomesophases (e.g., nematic, smectic) [1, 5].

1.2.1 The Lamellar Lyotropic Liquid Crystal Phases

The lamellar (Lα) lyotropic phase, also known as "neat phase", has the structure as shown in figure 1.2. It can be seen that in this phase the amphiphilic molecules are arranged in bilayer separated by water layers. The layers extend over large distances, usually of the order of several microns. Depending on the water content, the thickness of water layer can vary from approximately 10 ˚A to > 100 ˚A. The bilayer thickness is generally about 10-30% less than twice the length of an alltrans nonpolar chain. Usually, lamellar mesophases only exist down to 50%. When surfactant is below 50%, transition from lamellar phase to hexagonal phase or an isotropic micellar solution may occur. However, in certain extreme cases the lyotropic lamellar phases are exhibited in extremely dilute solution and, their parallel layers slide over each other easily during shear and hence lamellar phases are less viscous than the hexagonal lyotropic phases [5].

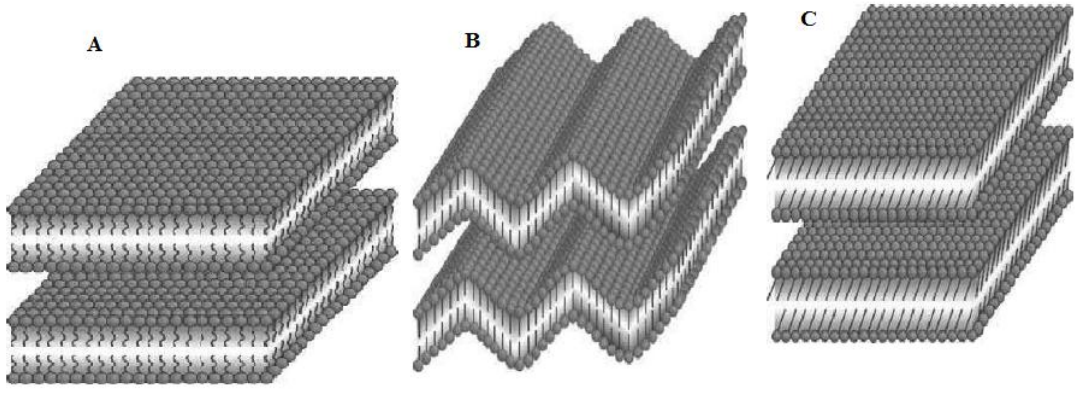

Figure 1.2: Sketch of the lamellar structure: (A) Lα phase, (B) ripple phase Pβ′ and (C) Lβ′ phase [5].

1.2.2 The Hexagonal Lyotropic Liquid Crystal Phases

In the hexagonal lyotropic liquid crystal phases, the cylindrical micelles are usually packed in the hexagonal array. Two well-established phase structures are identified; the hexagonal phase (H_1) (Figure 1.3a), and the reversed (or inverse) hexagonal phase (H_2) (Figure 1.3b). In the H_1 phase, the calamitic micelles of indefinite length are packed in a hexagonal array and separated by a continuous region. The diameter of the micellar cylinders is typically 10-30% less than twice the length of an all-trans nonpolar chain. Depending upon the contents of water and surfactants, the spacing between cylinders varies appreciably between 1 and 5 nm. Although hexagonal phase contains high water content, the phase is very viscous [5].

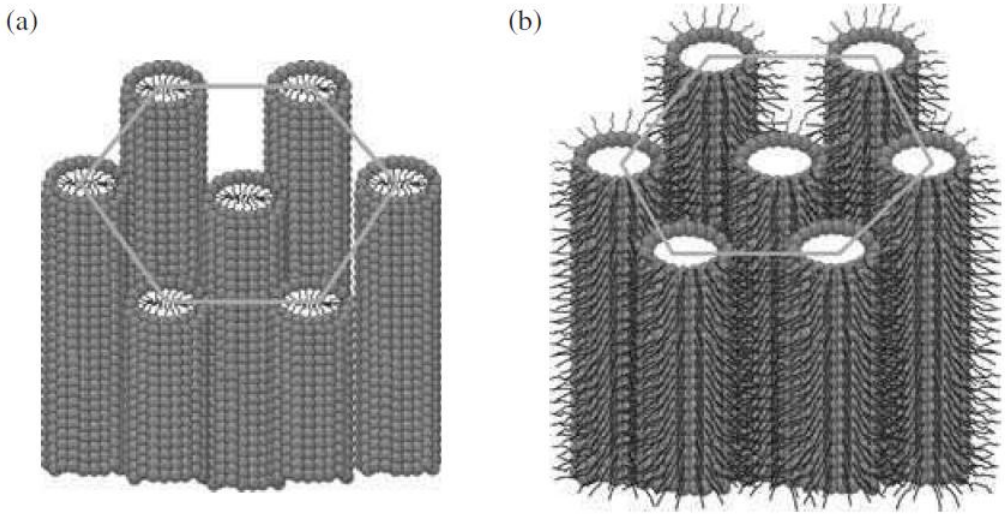

Figure1.3: Sketch of the hexagonal lyotropic liquid crystals phase structure: (a) direct; (b) inverted [5].

In the reversed hexagonal phase (Figure 1.6b), the hydrocarbon chains occupy the spaces between the hexagonally packed water cylinders of indefinite length. The water is contained within the cylindrical reversed micelles having a typical diameter of 1 to 2 nm.

The nonpolar chains occupying the remaining space overlap to bring the cylinders much closer together than in the hexagonal phase. The H_2 phase occupies much smaller region of the phase diagrams than the H_1 phase [5].

1.2.3 The Cubic Lyotropic Liquid Crystal Phases

The cubic lyotropic phases, also known as viscous isotropic phases, structurally are not as well characterized as the lamellar or hexagonal phases. In the most well known cubic phase there exists a cubic arrangement of molecular aggregates; these are similar to micelles (I_1 phase) or reversed micelles (I_2 phase). The cubic phases are extremely viscous; even more viscous than hexagonal phases. They are optically isotropic and so are often called the viscous isotropic phases [5]. Cubic gels can be prepared from other phases like lamellar or hexagonal which is depended on self assemblies of surfactant in solvent (concentration dependent) by simply expose aqueous phase (lamellar or hexagonal) to ultrasonic vibration. The manufacture of cubosomes is more complicated than other phases. The figure 1.4 represented the cubic lyotropic liquid crystal phase.

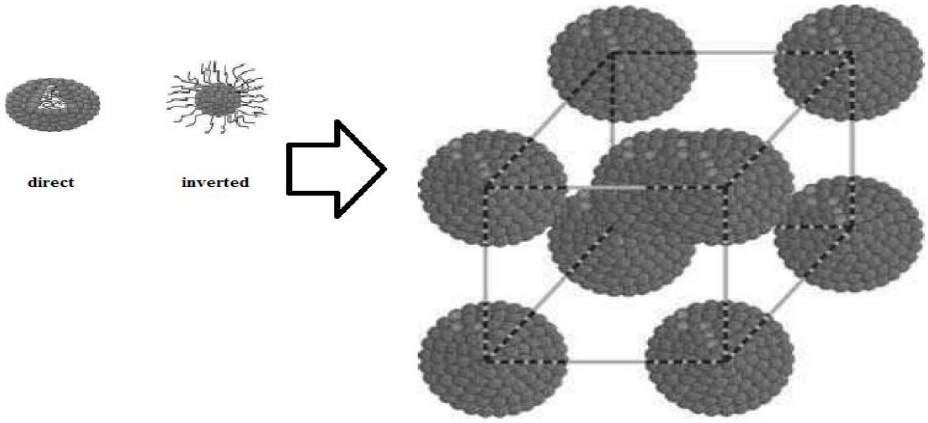

Figure 1.4: present the cubic lyotropic liquid crystal phase, direct and inverted micellar which are arranges them into body center cubic (bcc) phase.

1.3 Mechanism of self-assembly of surfactant in solvent

The mechanism of ordering in between the water molecules, based on the hydrogen bonds water molecules, plays an essential role in these effects [6]. In order to avoid such contacts, some amphiphilic molecular tend to locate at the air/water interface, with the head group (hydrophilic) in water and the tail (hydrophobic) in the air side of the interface, thereby forming an adsorbed layer of amphiphilic molecular. The Adsorption of amphiphilic molecules at the air/solution interface reduces the surface tension of water, thus the generic name surfactants (amphiphilic molecular). Similarly, surfactants adsorb on the solid walls of the flask containing the solution. The structure of an adsorbed layer of surfactant on a solid surface depends on the nature of the surface and of the surfactant [7-8]. As the amphiphilic molecular concentration in the solution is increased, the amount of amphiphilic molecules adsorbed at the air/solution interface (and on the walls of the flask containing the solution) increases up to the point where the interface becomes saturated by absorbed amphiphilic molecules. From this point, the concentration of the solution may be increased and the amphiphilic molecules dissolved in the aqueous phase may still be in a molecularly dispersed form. However, the free energy of the system increases with the concentration, due to the increasing number of unfavorable alkyl chain/water contacts together and forming micelle.

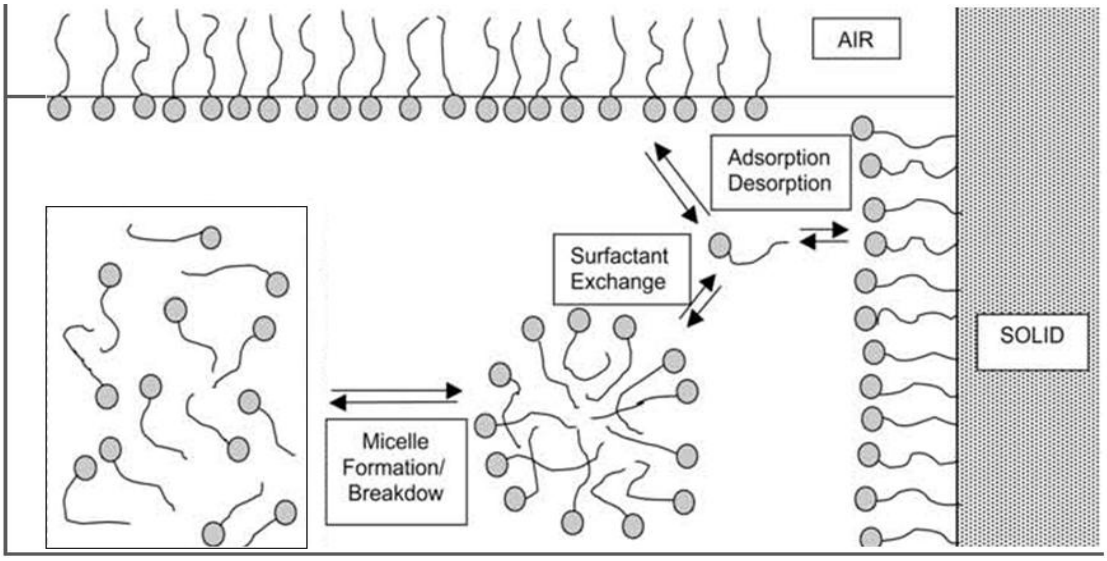

Figure 1.5: Mechanism of self-assembly in a surfactant.

1.3.1 Micelle formation

1.3.1.1 Theoretical Aspects

The reason behind surfactant self-assembly into micelles is the hydrophobic interaction between surfactant alkyl chains [9-10]. This interaction has its origin in the strong attractive interaction that exists between water molecules (hydrogen bond). Even though alkyl chain-water molecule interactions are attractive, they are energetically less favorable than interactions between water molecules [10-11]. As a result, when alkyl chains are immersed into water, the system tends to minimize its free energy by eliminating alkyl chain-water molecule contacts minimum possible. With surfactants, this results in the formation of micelles where the alkyl chains are in contact with one another, forming the micelle core. The head groups remains at the surface of the core, further reducing alkyl chain-water molecule contacts.

Several repulsive interactions oppose the formation of micelles [10, 12]. The main ones are the electrostatic interaction between head groups, the interaction arising from the packing of head groups at the micelle surface and of alkyl chains in the micelle core, and an interaction associated with residual alkyl chain-water molecule contacts at the micelle surface. The balance between attractive and repulsive interactions results in finite size micelles formation.

At a concentration very close to the CMC, the micelles are spherical or nearly spherical on a time-average basis. As the concentration is increased, the micelles may kept as spheroidal or grow and become oblate (disc like) or prolate (or elongated, cylindrical, or rod like), with the prolate shape much more often encountered than the oblate shape.

The micelle shape is determined by the value of the surfactant packing parameter P given by

$$P = \frac{v}{a_o\, l} \tag{1.1}$$

Where v and l are the volume and length of the hydrophobic moiety (alkyl chain) and a_o is the optimal surface area occupied by one surfactant at the micelle-water interface [1].

The volume of amphiphile can be calculated by following approximate relationship:

$$v = (27.4 + 26.9n) \tag{1.2}$$

Where n is the number of the atoms in organic molecular

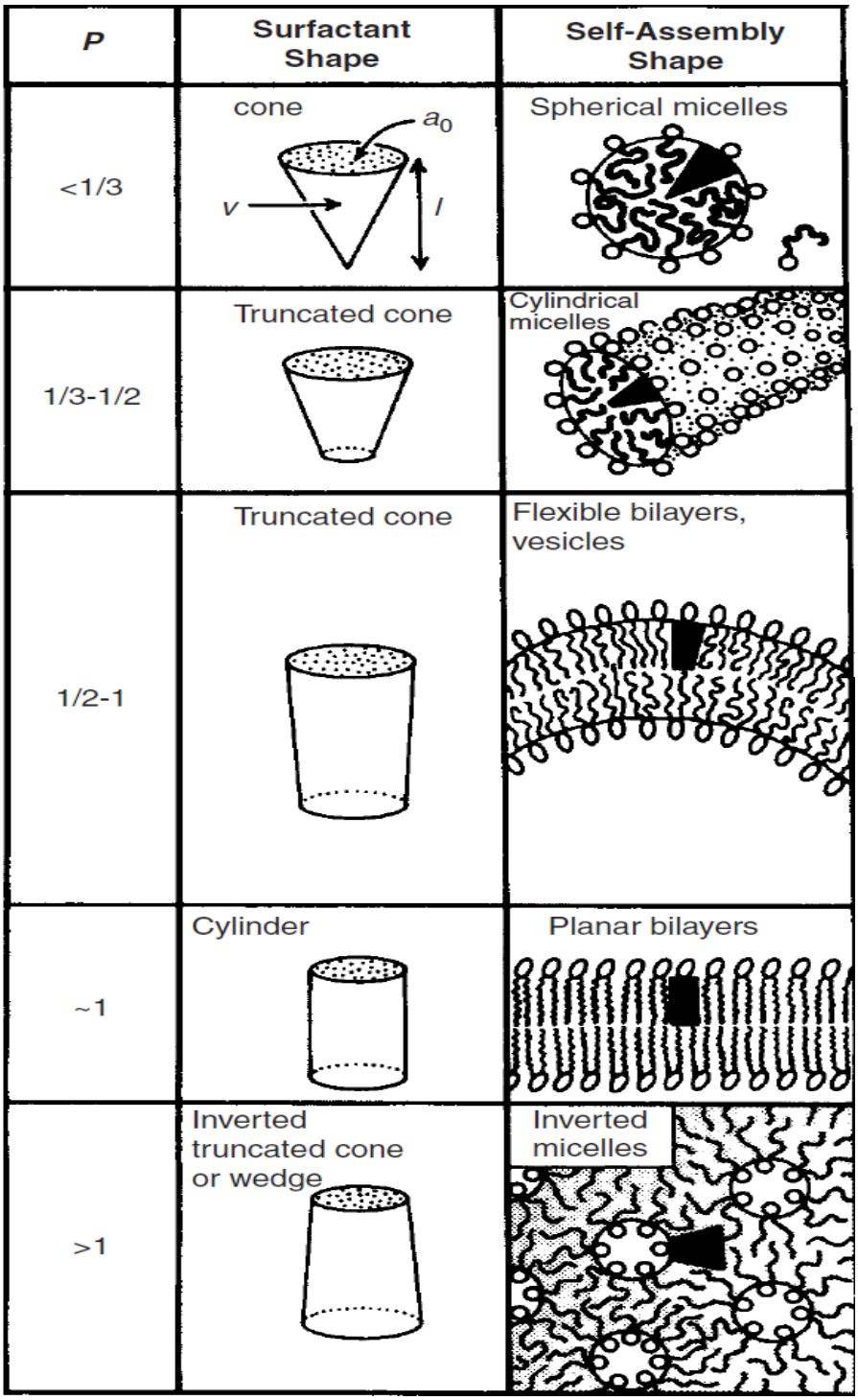

Figure1.6: Schematic represented of the shapes of the surfactant and self-assemblies for various values of the packing parameter.

1.3.1.2 Experimental Aspects

Micelles start forming in aqueous solutions of surfactant at concentration C > CMC (critical micellar concentration). The CMC is not a single concentration but rather a narrow range of concentration [14-15]. Its value slightly depends on the method of determination, reflecting differences in the way each measured property weighs micelles and free surfactants. The value of the CMC is determined mainly by the nature of the surfactant (ionic or nonionic) and by the length of its alkyl chain [16].

$$\text{Log}_{10}\ \text{CMC}=1.6 - 0.3n_c \qquad (1.3)$$

Where CMC is critical micellar concentration and n_c is the number of carbon atoms in alkyl chain.

1.4 Literatures review:

A report on preparation of lyotropic liquid crystal from Ternary system SDS/CTAB/ WATER were found in literature [17]. Lamellar phase was found in the high viscosity samples in which the cationic and anionic surfactant are in 1: 3 or 3: 1 stoichiometry. The viscosity increase is due to the salt can screen the repulsion between different charged head groups and thus reduces the effective size of surfactants and facilitates the spherical or rod likes micelles to be transformed to worm-like micelles which can form hexagonal or liquid crystal phases. In similar way Ghosh *et al.* [18] present a report on study of polyoxyethylene nonyl phenol (Igepal) in aqueous solution. The quenching process was exploited to estimate the aggregation number of surfactant monomer. In the Igepal series the micellar aggregation number systematically varied. From the dynamic light scattering studies in micellar solution the polydispersity of the medium and the diameter of the

micelles have been determined. It was concluded that the diameters of the micelles have been increased with increase in the molar mass of surfactants. A reasonable estimation of the surface area of the head group in different micelles has been attempted.

The first order transition between the normal hexagonal phase (Hα and lamellar gel phase (L_β, L_β., L_δ, type) in lyotropic liquid crystals of binary surfactant/water systems is reported in the literature. It was concluded that concluded that the mechanism for the phase transformation is view of topological structural transformations and a modification of the short-range order associated to the disorder/order transition of the configuration of the paraffinic chains. Bhowmik *et al.* [19] in 2005 presented a series of protic ionic salts were synthesised by a simple acid–base reaction from various pyridine derivatives and dodecylbenzenesulfonic acid in a common organic solvent and characterised in terms of their thermal and lyotropic liquid crystalline properties using various experimental techniques. All of them exhibited lyotropic liquid crystalline phases in toluene, methanol, acetonitrile, dimethyl sulfoxide and water. Their critical concentrations for the formation of biphasic solutions and concentrations for the formation of lyotropic solutions were quite broad depending on the dielectric constants of the solvents. Their lyotropic phases were identified as lamellar phases, since their textures exhibited, oily streaks and mosaic textures. They can potentially be used for many organic transformations, which may have implications in green chemistry. Glycolipids which are amphotropic liquid crystals forming lyotropic liquid crystals in aqueous solutions and thermotropic liquid crystals in their dry form were reported by Liao *et al.* [20] this study focused on the thermotropic properties of seven different neat glycolipids: four maltoside, two glucoside and one pyranoside lipids. He studies the dielectric susceptibility of these materials at frequency

range between <100 Hz and >1 MHz and temperature above 100^{o}c. The dielectric susceptibility of this materials vary from (60–120) basically proportional to the number of polar sugar heads. Kordell *et al.* [21] reported the study the dielectric permittivity of liquid crystals (8-CB), near the phase transitions. The results show significant changes (enhancement) of the dielectric permittivity of the liquid crystal near the smectic-to-nematic and nematic-to-liquid phase transitions attributed to structural changes of the relevant phases. Similarly Bauman *et al.* [22] studied the dielectric permittivity in the nematic and isotropic phases of 4−cyanophenyl−4'−n−octylbenzoate (8CPB) at frequency range from 50 kHz to 100 MHz. The relaxation process related to the rotation around the short molecular axis has been analyzed. They concluded that the dielectric measurements of 8CPB in the static electric field reveal the occurrences of antiparallel molecular association, although, as compared with 8CB, the ability to association is hindered because of the presence of the lateral C = O group. This fact, together with the high dipole moment of the 8CPB molecule, causes that the electric permittivity value of this liquid crystal is relatively high. Raicu *et al.* [23] studied the dielectric permittivity of yeast cells in the absence and presence of cetyltrimethylammonium bromide CTAB. The experimental permittivity and conductivity spectra of frequency were analyzed by means of the two-shell electrical cell model and the electrical phase parameters of cells were subsequently evaluated. Both the cytoplasm and vacuole conductivities interior decreased drastically by treating the cells with surfactant. The apparent capacitance of the plasma membrane increased systematically from (0.65 μF/cm^2), for untreated cells, up to about (0.75 μF/cm^2, at 0.3 mM) CTAB. Within the accuracy of the data, the specific capacitance of the vacuole membrane was nearly constant (0.544±0.021 μF/cm^2) over the

whole surfactant concentration range. Also, the cytoplasm permittivity remained constant at 64.3±4.5 Buchner *et al.* [24] in 2005 presented a report on dielectric relaxation of ionic surfactant solutions and discussed the comparative results for cationic (alkyltrimethylammonium halides, C_nTAX) and anionic (sodium dodecylsulfate, SDS) surfactants. Whereas the surface of SDS micelles is strongly hydrophilic with adsorbed counter ions generally separated by a layer of water molecules, the surface of C_nTAX micelles is essentially hydrophobic and bound halide ions are directly attached. His concluded that the SDS surfactant having faster responding to the external electrical fields than the cationic surfactant this clear in relaxation peak. Vijayaraghavan et al. [25] reported the hysteresis in lyotropic liquid crystals by using DSC device. He studies this for (SdS)/decanol/water system for two different concentrations of the constituents. It was found that system exhibits calamitic nematic (Nc), isotropic (I) and hexagonal (H) phases on heating from the room temperature. On heating the samples, the DSC thermograms exhibit two peaks which can be related to the reported Nc-I and I-H phase transition temperatures. However, on cooling from a high temperature they do not exhibit any peak. Ono *et al.* [26] in 2005 present a first-principles study of the dielectric properties of a NaCl crystal and ultrathin NaCl films under a finite external electric field. Our results show that the high-frequency dielectric constant of the films is less affected by the finite-size effect from crystal surfaces and is close to that of the crystal, whereas the static one is sensitive to the thickness of the film because of the thick buffer region where ionic displacements due to the electric field are not as homogeneous as those in the bulk.

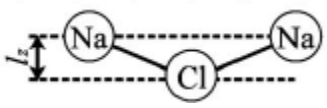

Figure 1.7: represented ultrathin NaCl films under a finite external electric field

This is consistent with the induced charge due to the electric field, in which no significant distinction in the induced charge around the Cl ions is observed between the thick films and thin films nor between the films and the crystal. On the other hand, the static dielectric constant is sensitive to the thickness of the film because of the thick buffer layers where the ionic displacements due to the applied electric field are not homogeneous. Other alkali-metal halide materials are expected to show similar properties to those of NaCl and an investigation of them is in progress.

CHAPTER 2

Experimental methods and characterization techniques

2.1 Selection of materials

A variety of material have been used and studied to understand the dielectric properties of the lyotropic liquid crystal systems. The selection of material used plays an important role on the performance and device application. There are many types of amphiphilic molecules which is forms lyotropic liquid crystals phase aanionic, cationic non-ionic and zwitterionic. On the basis of polarizability criteria ionic amphiphiles posses higher polarization than that of the non-ionics and hence result higher dielectric permittivity [27]. This study devoted to examine the structural and dielectric responses of the ternary mixture of sodium dodecyl sulfate (SDS), cetyltrimethylammonium bromide (CTAB) and water at various concentrations. Both the chemical were procured from Loba Chemie and used as received without any further purification. The chemical structures, physical and chemical properties of these materials are shown figure 2.1 and listed in Table 2.1.

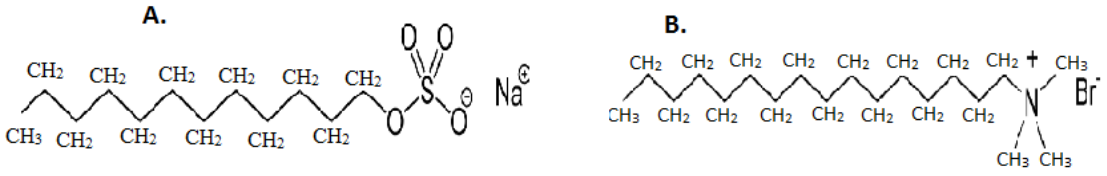

Figure 2.1: Chemical structure of surfactant (A) SDS and (B) CTAB [28-29].

Table 2.1: Physical and chemical properties of surfactants

Properties	SDS	CTAB
Molecular formula	$NaC_{12}H_{25}SO_4$	$C_{19}H_{42}BrN$
Molecular mass	288.372 $gmol^{-1}$	364.45 $gmol^{-1}$
Melting point	206 °C	237–243 °C
Appearance	white powder	white powder

2.2 Preparation of lyotropic liquid crystals:

Lyotropic liquid crystals have been prepared by mixing two types of surfactants SDS and CTAB in aqueous media (water) in different weight concentration as describe below in table (2.2).

Table 2.2: Weight fraction for each sample

Sample no.	Weight of SDS	Weight of CTAB	Weight of water (solvent)	Weight concentration
	All the sample having 0.001 mole from each SDS and CTAB			
Sample 1	0.28 g	0.36 g	5.87 g	10%(SDS,CTAB)
Sample 2	0.28 g	0.36 g	3.7 g	15%(SDS,CTAB)
Sample 3	0.28 g	0.36 g	2.61 g	20%(SDS,CTAB)
Sample 4	0.28 g	0.36 g	1.53 g	30%(SDS,CTAB)
Sample 5	0.28 g	0.36 g	0.65 g	50%(SDS,CTAB)

In typical procedure all the components were mixed in the glass vial in appropriate amount followed by the heat treatment (up to 50^0C) to give proper diffusion and

homogeneity. The heating and cooling cycle were repeated for three times to ensure the proper diffusion and mixing molecular level. The prepared samples were left at room temperature for 48 hour to recover the thermal equilibrium and phase. Same procedure was employed to fabricate the samples with 15, 20, 30 and 50 wt%. The ternary phase diagram for these systems is presented in the figure 2.2 [17].

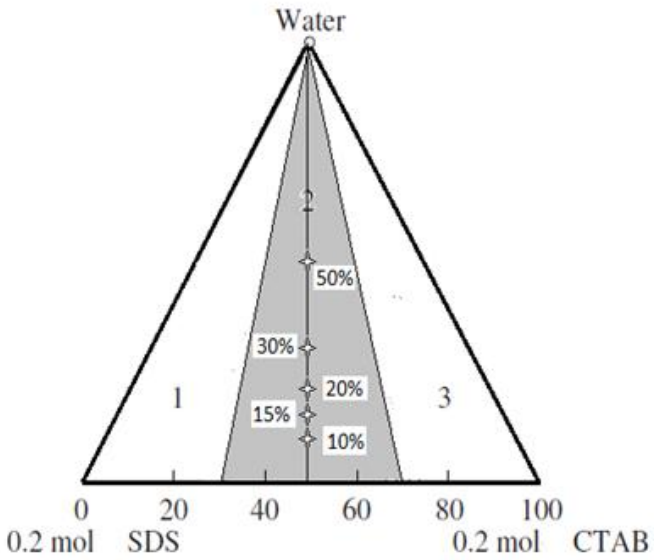

Figure 2.2: Pseudo ternary phase diagram of SDS/CTAB/H_2Omixture system at 40°C. Phases in regions 1 and 3 are transparent and homogeneous, in 2 is sedimentary and turbid.

The flow chart for the methodology is given below

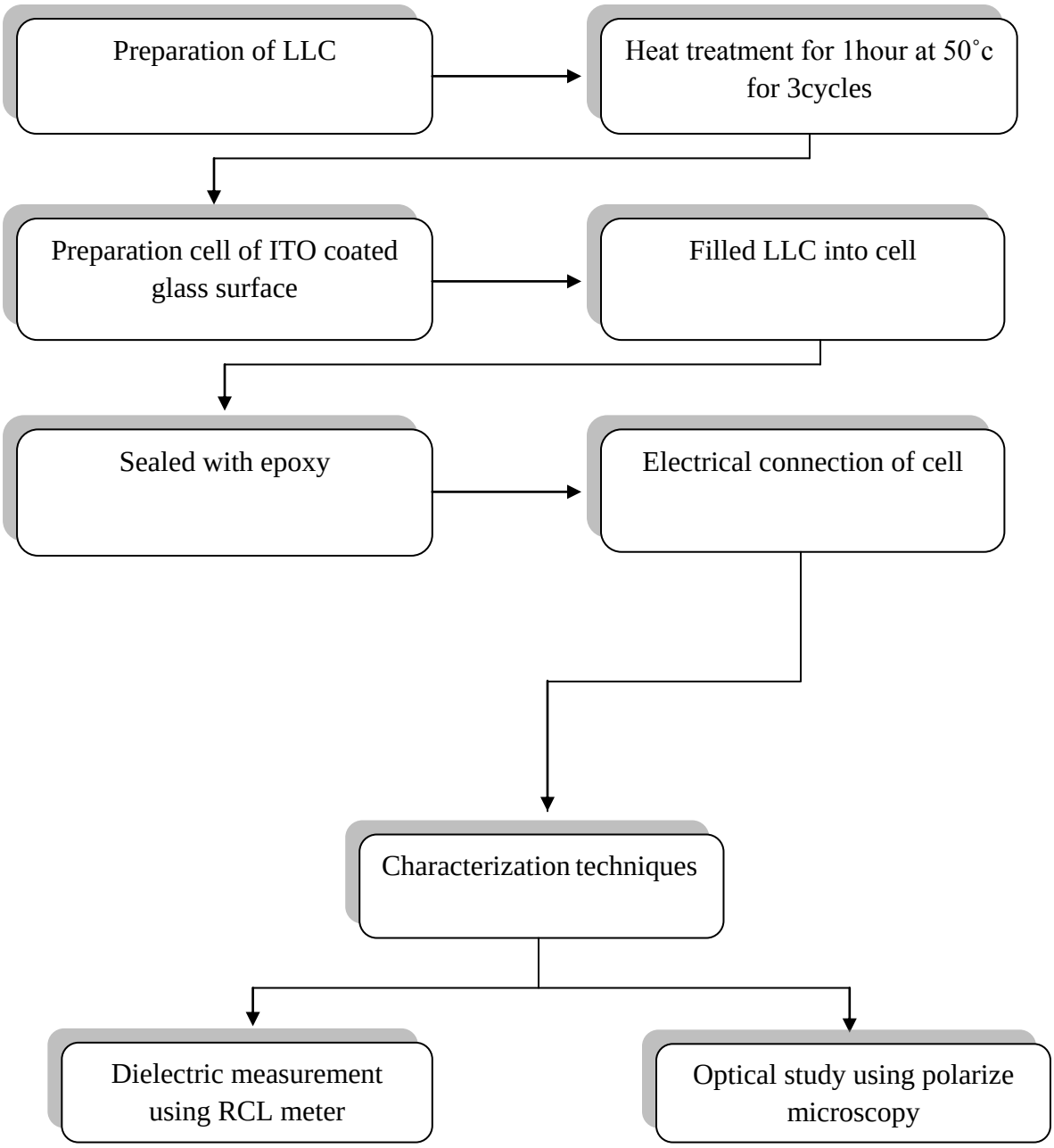

2.3 Sample Cells Assembly:

A lyotropic liquid crystals samples cells were prepared using conducting indium tin oxide (ITO) coated glass substrates. These ITO coated glass substrates were highly transparent with resistivity of the order of few 140-180 ohm-m. The substrates were initially washed with soap solution, rinsed with acetone (purity 99.9%), distilled water and then dried in a vacuum furnace. The conducting sides of these ITO coated glass substrates were joined together and separation between the substrates was maintained with the help of rough spacer thickness about 20μm. The samples were filled in between the fabricated cell. The sample cell was sealed with optical adhesive and epoxy .The electrical connections were made with indium solder. The empty cell was calibrated with standard acetone before filling. The cell assembly is shown in figure 2.3.

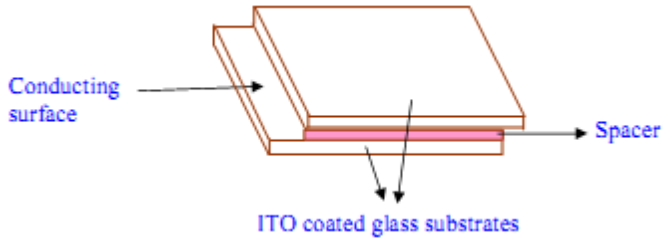

Figure 2.3: Assembly of ITO cell

2.4 Experimental Techniques:

2.4.1 Thermo-optical measurements:

In order to study the lyotropic liquid crystal texture morphology and phase transition temperatures, Olympus polarizing microscope (Model- BX51P) and Linkam temperature programmer cum hot stage (Model TP94 and THMS 600) was used. The microscopic optical textures were captured through the charge coupling device (CCD) digital camera (Olympus DP 12 JAPAN) fitted on polarizing microscope and interfaced to a computer. The assembly for the thermo optical measurements presented in the materials research laboratory is show below

Figure 2.4: Optical polarizing microscope and thermo-optical set up

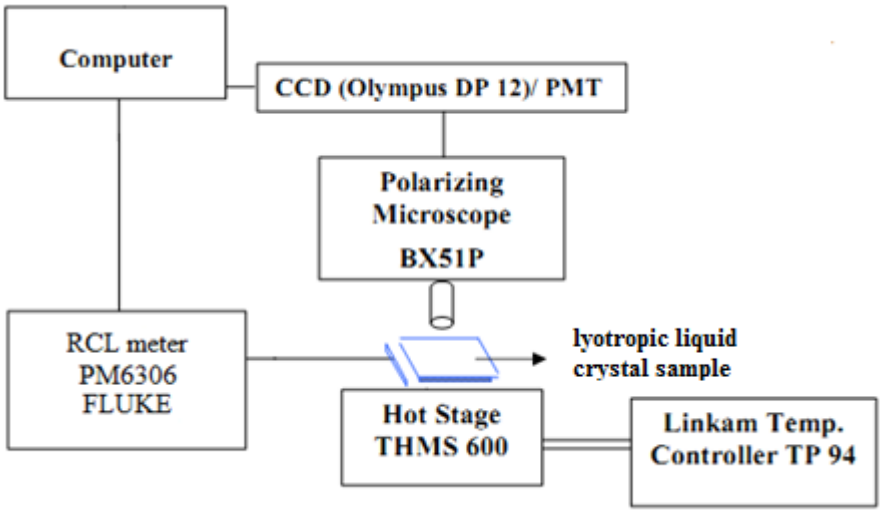

Figure 2.5: Block diagram of the experimental set-up to study textures and dielectric properties of lyotropic liquid crystal

2.4.2 Dielectric measurements

The dielectric measurements were carried out using a programmable automatic RCL meter (FLUKE PM 6306 showed in figure 2.5) in the frequency range 50Hz to 1MHz. The cell was calibrated using air and acetone as standard references. The frequency and bias dependence of the real and imaginary parts of the complex dielectric permittivity have been studied in detailed at different temperatures. The dielectric properties of the lyotropic liquid crystal were taken at zero DC voltages. Dielectric spectroscopy technique measures the dielectric properties of a medium as a function of frequency, temperature. In the case of lyotropic liquid crystal medium, dielectric spectroscopy is a powerful technique that is capable of probing the molecular motion and the electric properties.

Figure 2.6: represented the RCL meter model (PM 6306 FLUKE) [30].

The calculation of dielectric constant of lyotropic liquid crystals can be done through equations listed below:

$$C_{effective} = \frac{C_{acetone} - C_{air}}{1.254} \quad (2.1)$$

$$\varepsilon' = \left(\frac{C_{LLC} - C_{air}}{C_{effective}}\right) + 1 \quad (2.2)$$

$$\varepsilon'' = D \times e' \quad (2.3)$$

Where $C_{acetone}$, C_{air} and C_{LLC} are the capacitors values in acetone, air and lyotropic liquid crystals mediums respectively. D is Dissipation factor, ε' is the dielectric constant of the material, also known as the relative dielectric permittivity, and it is used to define the ability of the material to store electrical charge. ε'' is the imaginary part, which is related to the loss and known as the dielectric loss. The complex dielectric properties, the relative permittivity (ε') and the loss factor (ε'') are determined by scans as a function of

frequency. The displacement of the charge by applying the electric field is called "polarization". The dielectric properties of a material are defined by a complex dielectric permittivity, ε* which can be calculated through equation below.

$$\varepsilon * = \varepsilon' + i\,\varepsilon'' \qquad (2.4)$$

CHAPTER 3

Results and discussions

This chapter summarized results obtained from the various characterization techniques like optical microscopy and dielectric spectroscopy and discussion on some fundamental aspects.

3.1 Thermo-optical analysis:

Figure 3.1 represents the optical texture of the all samples at 30^0C, 45^0C and 60^0C respectively. It was observed that these ternary mixtures are stable 45^0C (represents the parent phase it exhibit at 30^0C) and shows the phase transition at 60^0C. However no exact information about the phase has been observed from these samples and need further experimentation like small angle X-ray spectroscopy analysis to predict the exact LLC phase. The phase transition observed in this thermo-optical analysis further confirmed from dielectric spectroscopy and correlated to understand its effect on the molecular orientations and ordering of the systems.

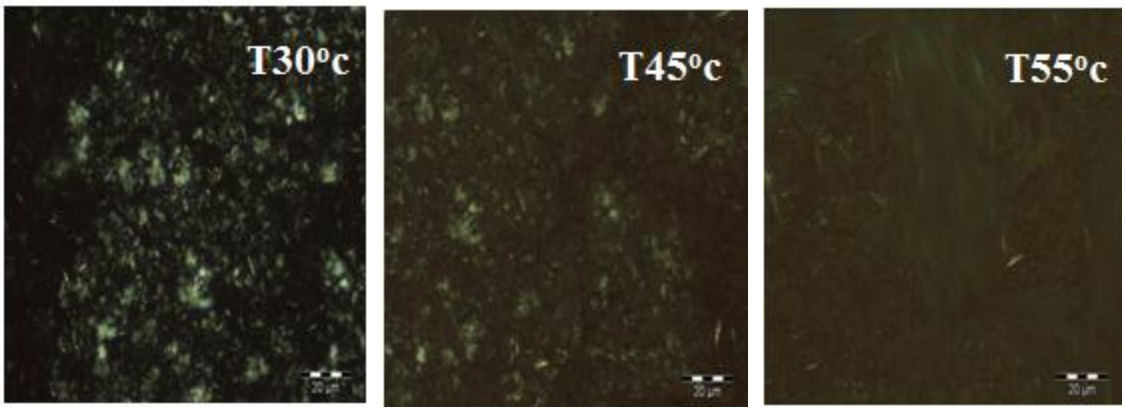

a

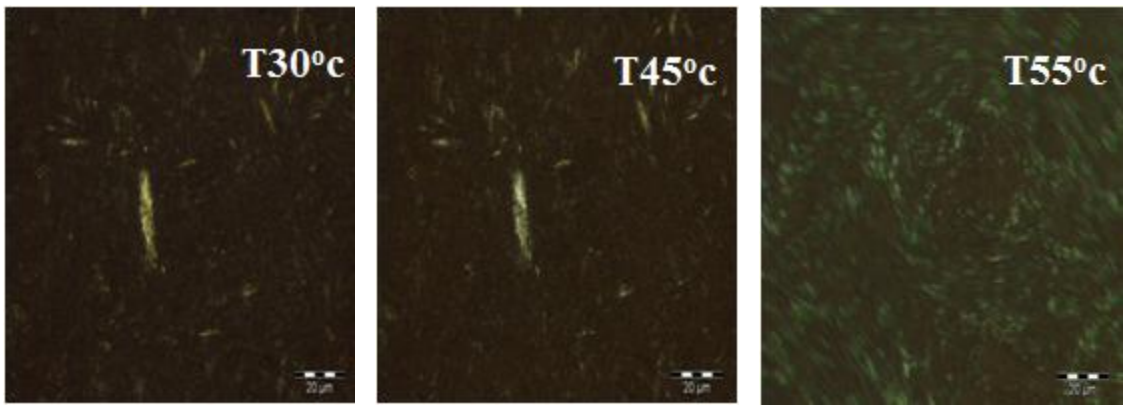

b

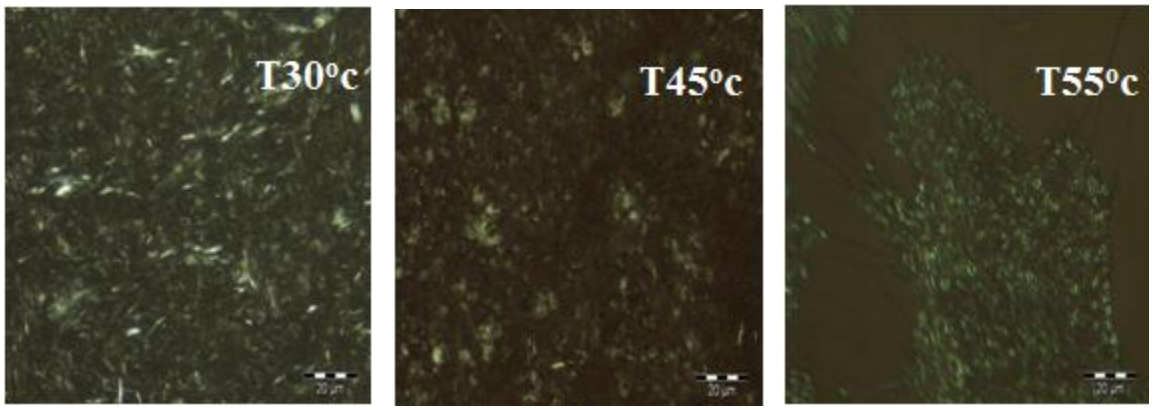

c

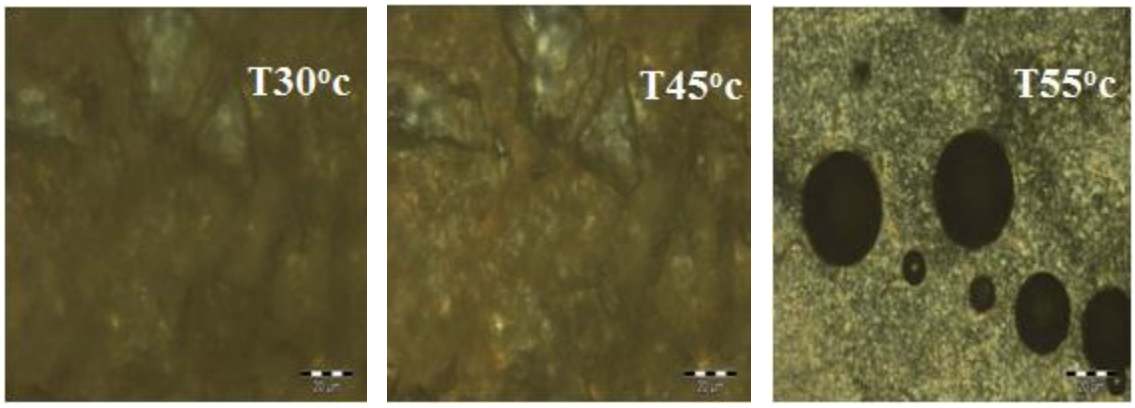

d

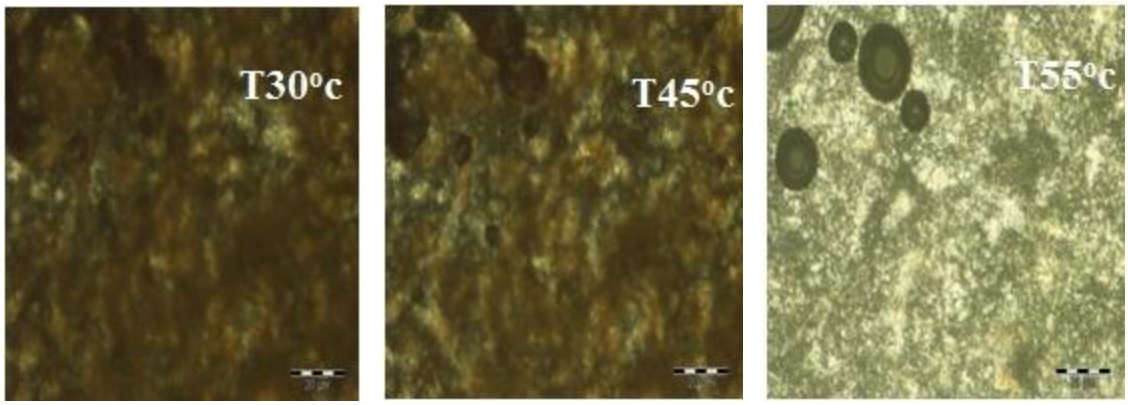

e

Figure: 3.1 Optical texture at various temperature (a) sample 1 (b) sample 2 (c) sample 3 (d) sample 4 (e) sample 5

3.2 Dielectric spectroscopy:

3.2.1 Frequency dependent dielectric spectroscopy

Frequency dependent dielectric spectroscopy for the all five samples is shown in (Sample1, 2, 3, 4, and 5) figure 3.2. In general all the samples demonstrate well defined exponential decay behavior with the progression of the frequency up to 1KHz which further become very less and frequency invariant at higher frequency region in heating cycle. Large dispersion in the permittivity was also noticed with the increase in the temperature. The permittivity was found higher at 30^0C which further fall to the lower magnitude at higher temperature (60^0C) for all the systems. The corresponding loss for the samples was noticed low in the low frequency zone which further show maxima near 300 Hz and again depicts to the lower value at higher frequencies. Single relaxation peak have been observed in all the samples which could be corresponds to the Cole-Cole process. In cooling cycle all the samples represents the same exponential behavior as

heating cycle with the progression of frequency. The shift in relaxation frequency towards lower side has been seen in cooling conditions. It is interesting to note that the under cooling condition samples did not reach to the actual magnitude of the permittivity as we observed at room temperature in heating cycle. Which may be due to the fact that with the heating samples undergoes same phase transition near 60^0C and did not recovered to the ordered phase or required more time to reach the thermal equilibrium. This effect is further explained in detail in temperature dependent spectroscopy and correlated with other experimental findings exist in the literature.

Heating cycle

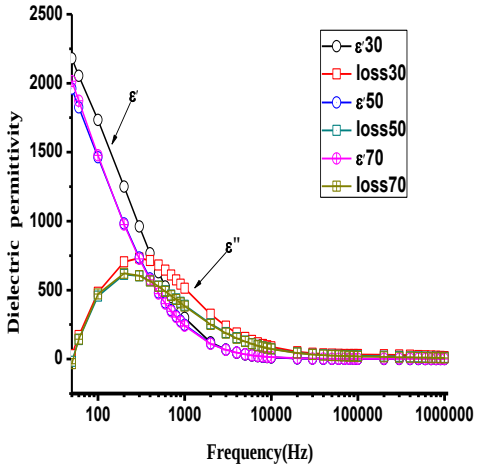

Cooling cycle

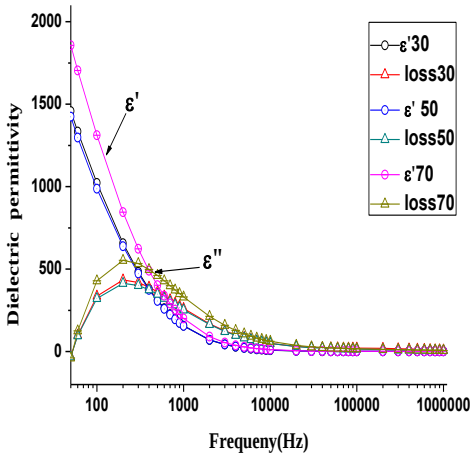

Sample (1): 10:90 wt%

Heating cycle

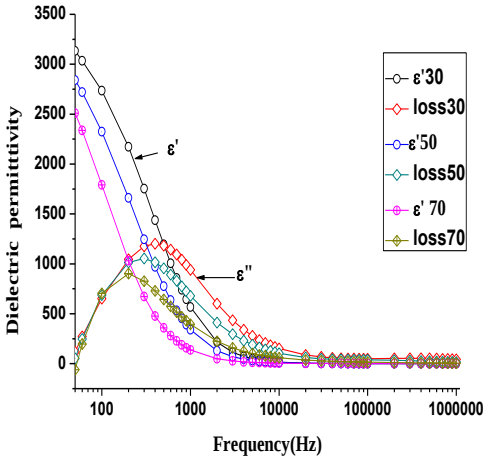

Cooling cycle

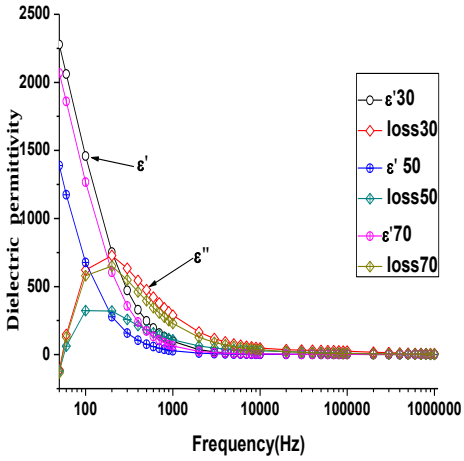

Sample (2): 15:85 wt%

Heating cycle

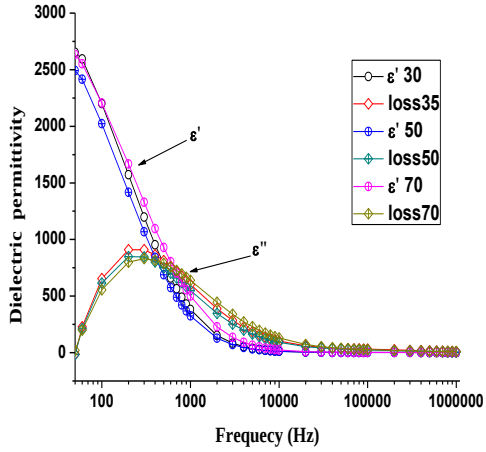

Cooling cycle

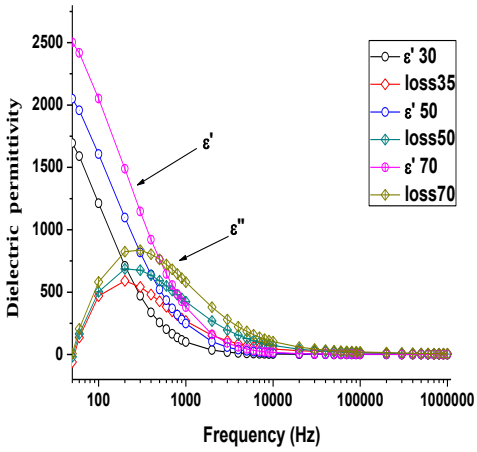

Sample (3): 20:80 wt%

Heating cycle

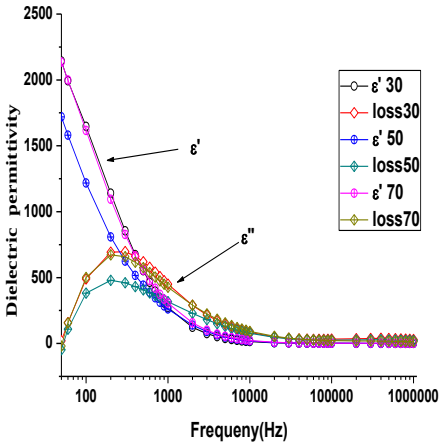

Cooling cycle

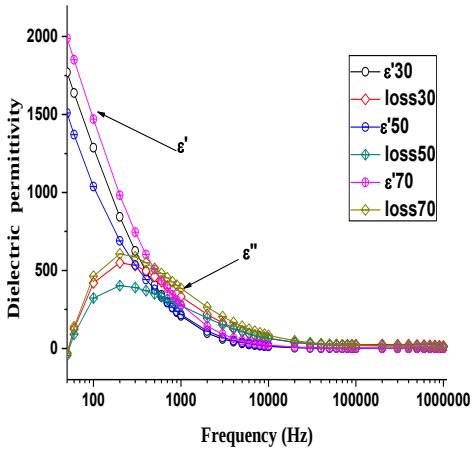

Sample (4): 30:70 wt%

Heating cycle

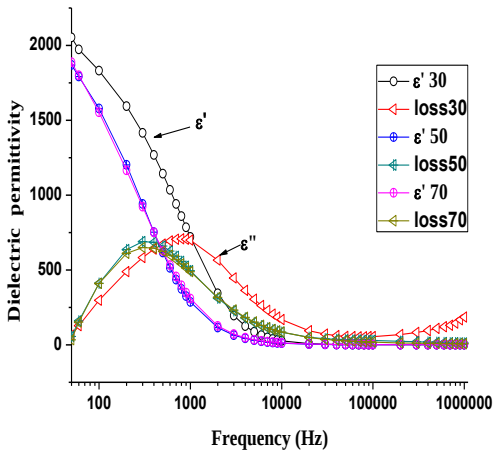

Cooling cycle

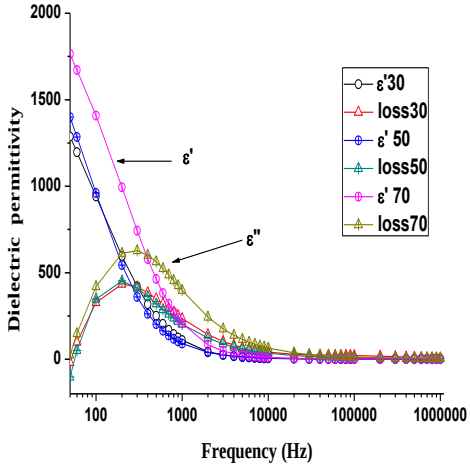

Sample (5): 50:50 wt%

Figure 3.2: Frequency dependent dielectric spectroscopy at different sample concentration.

3.2.2 Temperature dependent spectroscopy

The temperature dependent variation of the dielectric constant is shown in figure 3.3 at frequency 50Hz. During heating cycle the dielectric permittivity decrease with increase temperature from temperature range (30˚c to 45˚c), however the fluctuation have been observed near 60^0C (phase transition point) which is also in good agreement with the thermo-optical analysis. In cooling cycle the dielectric permittivity decreased drastically up to 50˚c and become almost constant with further cooling to 30^0C. Such behavior hints about the thermals hysteresis in the sample. In general perspectives when we heat the LLC mixture the size of the micelles decreased with the increase in the temperature which further leads to the phase transition in the systems as the surface area of the micelles change and system become micellar than that of liquid crystalline. We believe that such phenomena is taking place in these ternary mixture as we observed that continuum decrease in permittivity and phase change at 60^0C responsible for the thermal hysteresis in these systems.

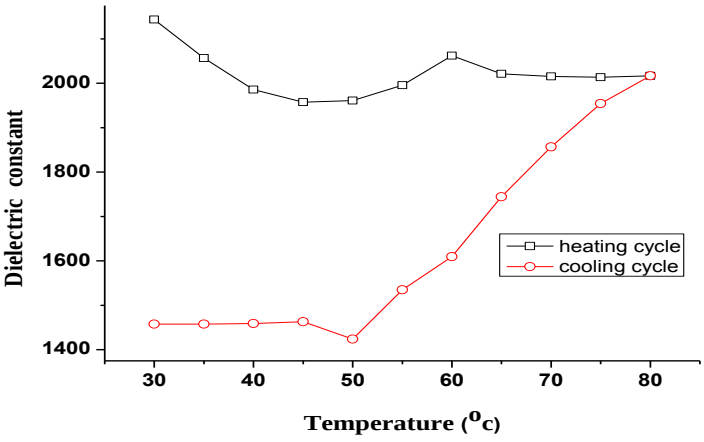

Sample 1

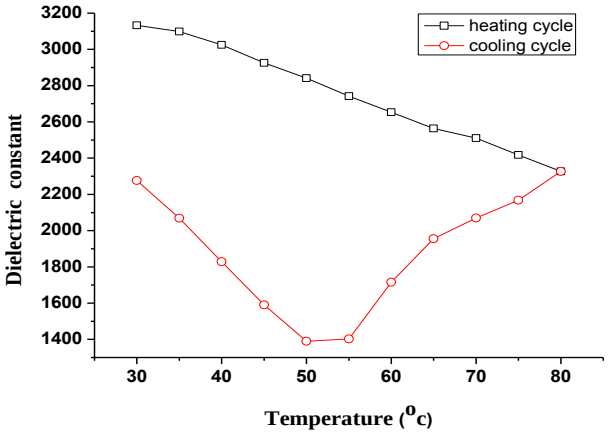

Sample 2

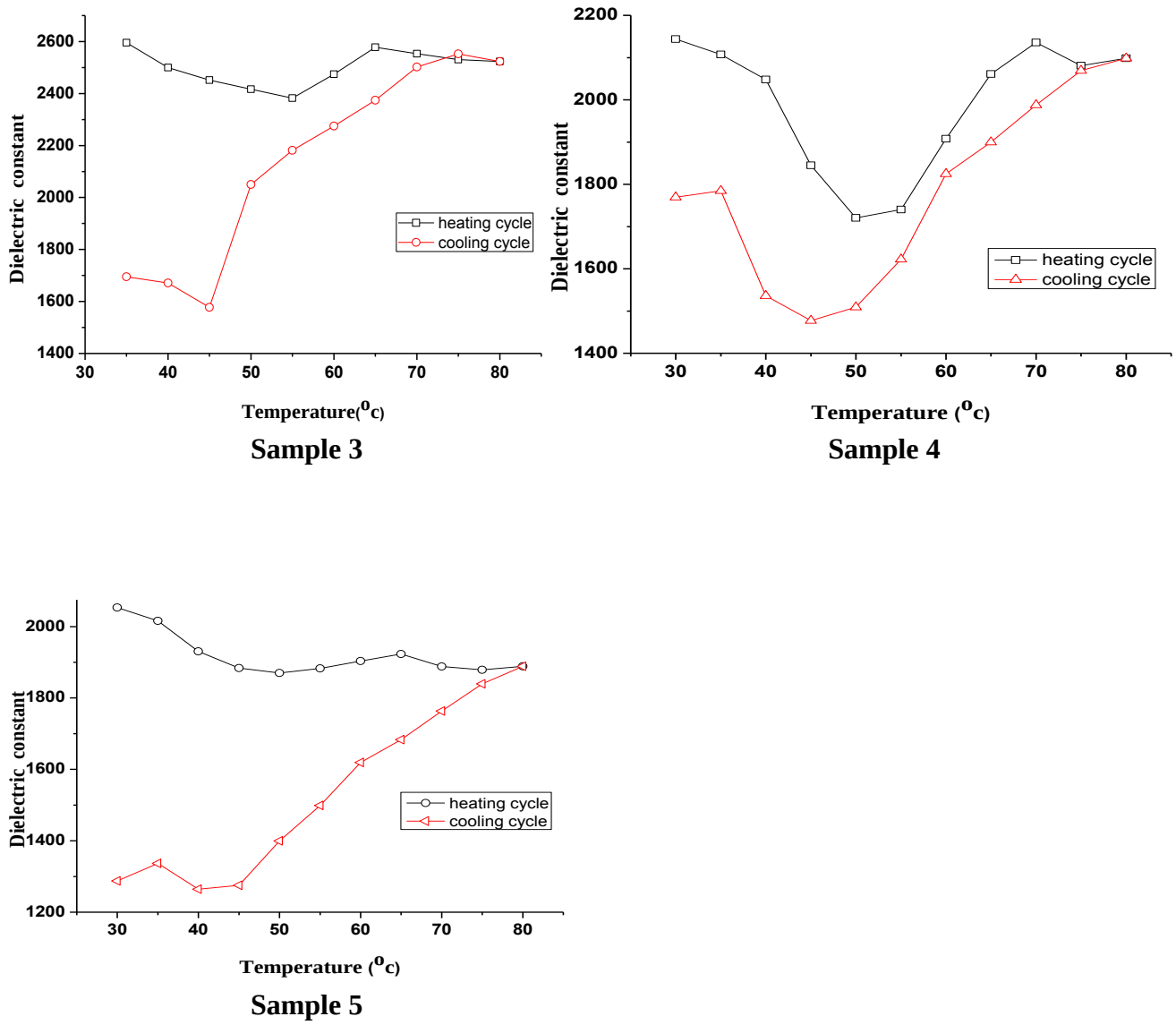

Figure 3.3: Temperature Vs dielectric permittivity under different heating and cooling cycles.

It was noticed that sample 3 and 5 also exhibited the same behaviour of permittivity and phase transition with the temperature variation. Instead of this sample 2 procured maximum magnitude of the permittivity than that of other samples at 30^0C. Continues decrease in the permittivity was observed with the increase in the temperature up to 80^0C.

There is no transition have been observed near 60^0C like the sample 1, 3, 4, and 5. Thought this sample shows the melting of the texture in the thermo-optical studies. Sample 4 shows some unusual behavior as we saw the defused transition in this case which may be due to the less ordering in the sample.

3.2.3 Concentration dependent spectroscopy

Figure 3.4 demonstrate the variation of dielectric constant with concentration at varying temperature (30˚c, 45˚c, 60˚c and 75˚c) at 50Hz. Sample procured 15:85 wt% concentration reflect the higher magnitude of the permittivity at all temperature except 75^0C. We study the dielectric constant in four temperature range. It was observed that the large dispersion in the permittivity is in the lower concentration zone (10- 30 wt %), however at higher concentration of surfactant the permittivity is almost constant. It was also worth noting that the higher concentration zone is thermally stable than that of the lower one.

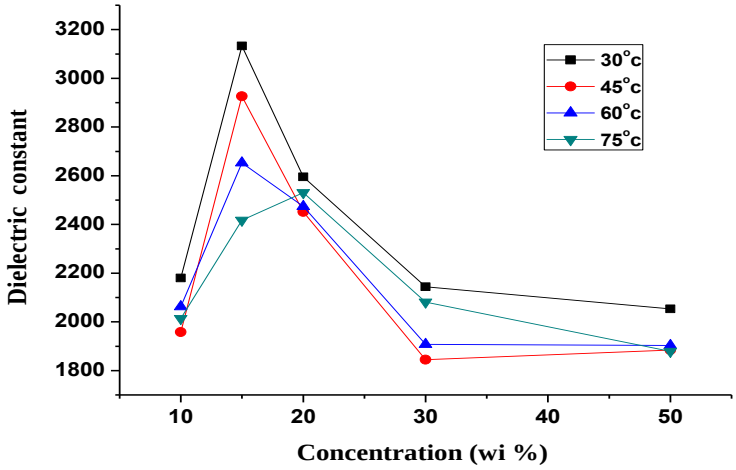

Figure 3.4: variation of dielectric permittivity with concentration at 50Hz.

CHAPTER 4

CONCLUSIONS

In summary we have introduced novel approach of preparing lyotropic liquid materials and investigated their dielectric behavior. The major conclusions of this work are as follows:

- The thermo-optical analysis hints about the optical anisotropy in these systems with the signatures of the liquid crystallinity, however, SAXS analysis will give the exact understanding of the LLC phases. These systems are found stable up to 55^0C as we observed first phase transition near 60^0C.
- All sample shows higher dielectric permittivity in the lower frequency region along with very less loss and single relaxation peak may be corresponding to the Cole-Cole relaxation process. Large dispersion in permittivity has been observed in these systems at the expense of temperature variation in the frequency dependent studies, which may be associated with the change in the optimal area and ordering of the micelles.
- The temperature dependent dielectric studies shows decrease in the permittivity with the increasing in the temperature, however, fluctuation near 60^0C owes to the phase transition. Such behaviors attributed to the unpacking of LLC structures to the micellar phase or solution at phase transition which takes time to reach thermal equilibrium when cooled back to the room temperature those materials do possess thermal hysteresis behavior.
- These LLC Mixtures are expected to find application on electrolytic capacitor due to their high dielectric permittivity.

References

1. A. M. Neto and S. A. Salinas, *in the physics of lyotropic liquid crystals phase transitions and structural properties*. Oxford University Press Inc (2005).

2. S. Chandrasekhar, *In Liquid Crystals*, 2nd Ed, Cambridge University Press (1977).

3. P.M. Chaikin and T.C. Lubensky, *Principles of condensed matter physics*, Cambridge university press (1992), Chapter 2.7 (page 58-70).

4. L Vicari, *In Optical Applications of Liquid Crystals*, Institute of Physics Publishing Bristol and Philadelphia (2003).

5. S. Singh, *in liquid crystals fundamentals*, World Scientific Publishing Co. Pte. Ltd (2002).

6. G. Yu, Z. Yang, M. Ameri, D. Attwood, J.H. Collett, C. Price and C. Booth, J. Phys. Chem. B 1997, **101**, 4394.

7. G. G. Warr, Opinion Colloid Interface Sci. 2000, **5**, 88.

8. S. Manne, T.E. Schäffer, Q. Huo, P.K. Hansma, D.E. Morse, G.D. Stucky and I.A. Aksay, Langmuir 1997, **13**, 6382.

9. C. Tanford, Proc. Natl. Acad. Sci. USA (1979), **76**, No. 9, pp. 4175-4176.

10. N. T. Southall, K. A. Dill, and A. D. Haymet, J. Phys. Chem. B (2002), **106**, 521-533.

11. K. Lum, D. Chandler and J. D. Weeks, J. Phys. Chem. B (1999), **103**, 4570.

12. R. Nagarajan and E. Ruckenstein, Langmuir (1991), **7**, 2934.

13. A. Shiloah and D. Blankschtein, Langmuir (1998), **14**, 7166.

14. Y. Moroi, *Micelles: Theoretical and Applied Aspects*, Plenum Press, New York, (1992).

15. P. Mukerjee, *Adv. Colloid Interface Sci*. (1967), **1**, 241.

16. K. Holmberg, D. O. Shah and M. J. Schwuger, *Handbook of applied surface and colloid chemistry Volume 1 – 2*, John Wiley & Sons Ltd (2002).

17. S. Zhang and H. N. Teng, Colloid Journal, (2008), **70**, No. 1, pp. 105–111.

18. S. K. Ghosh, P. K. Khatua and S. C. Bhattacharya, *J. Mol. Sci.* (2003), **4**, 562-571.

19. P. K. Bhowmik, A. K. Nedeltchev and H. Han, Liquid Crystals (2008), **35**, No. 6, 757–764.

20. G. Liao, S. K. Zewe, J. Hagerty, R. Hashim, S. Abeygunaratne, V. Vill and A. Ja'kli, Liquid Crystals (2006), **33**, No. 3, 361–366.

21. M. Kordell, T. Lawson, C. Prayaga and L. Ujj, Department of Physics, University of West Florida, Pensacola, FL.

22. D. Bauman, J. Jadzyn, E. Wolarz, A. Modlinska, and R. Dabrowski, OPTO−ELECTRONICS REVIEW (2010), **18**(1), 63–70.

23. V. Raicu, C. Gusbeth, D. F. Anghel and G. Turcu, Biochimica et Biophysica Acta (1998), **1379**, 7–15.

24. R. Buchner, C. Baar, P. Fernandez, S. Schrfdle and W. Kunz, Journal of Molecular Liquids (2005), **118**, 179– 187

25. D. Vijayaraghavan, Mol. Cryst. Liq. Cryst. (2011), **547**: pp. 189=[1879]–194=[1884].

26. T. Ono, K. Hirose, Physical Review B (2005), **72**, 085105

27. S. O. Kasap: *Principles of electronic materials and devices*, the McGraw-HiII Companies (2006).

28. http://en.wikipedia.org/wiki/File:Sodium_laurylsulfonate_V.1.svg (access in 4-6-2012)

29. http://upload.wikimedia.org/wikipedia/commons/3/36/Cetrimonium_bromide.png (access in 4-6-2012)

30. http://www.fluke.com/fluke/usen/Bench-Instruments/RCL-Meters/PM6306-&-PM6304.htm?PID=56500 (access in 1-6-2012)